Characterization of Polyamide 6 Made by Reactive Extrusion. II. Analysis of Microstructure

P. R. HORNSBY* and J. F. TUNG

Department of Materials Technology, Brunel University, Uxbridge, Middlesex UB8 3PH, United Kingdom

SYNOPSIS

Consideration is given to the characterization of microstructure in polyamide 6 prepared by polymerization of ε-caprolactam in a corotating twin-screw extruder. Results obtained by FTIR, WAXD, DSC, and DMTA are discussed in terms of the molecular mass of the polymer, the thermal history of the material, and the influence of residual monomer.

INTRODUCTION

A previous investigation considered the preparation of polyamide 6 (PA6) by the catalyzed anionic polymerization of ε-caprolactam in a corotating twin-screw extruder.[1] It was shown that, using an appropriate catalyst and activator system together with an optimized screw profile and operating conditions, high polymer could be produced with an average machine residence time of about 90 s. Molecular mass and residual monomer level were strongly influenced by screw speed. Mechanical properties compared favorably with commercial PA6 made by hydrolytic polymerization, with notched Izod impact strength and elongation at break being significantly higher for material produced by reactive extrusion.

This article considers the effects of processing history and material composition on microstructure of the materials produced. In this respect, previous work has established the existence of two crystalline forms of PA6, an α-phase and a thermodynamically less stable γ phase, giving rise to wide angle X-ray diffraction (WAXD) peaks at $\Theta = 19.6°$ (α_1), 23.5° (α_2), and 21.3° (γ), respectively.[2] In addition, differential scanning calorimetry (DSC) was used to study the effects of processing conditions and recrystallization rate on the thermal properties of PA6 fibers and yarns.[3]

* To whom correspondence should be addressed.

Journal of Applied Polymer Science, Vol. 54, 899–907 (1994)
 CCC 0021-8995/94/070899-09

EXPERIMENTAL

An earlier article discussed experimental procedures used for the preparation of PA6 by anionic polymerization of ε-caprolactam in a corotating intermeshing twin-screw extruder.[1] In the present study, consideration is given to the structural analysis of polymer prepared in this way at specified screw speeds ranging from 50 to 150 rpm, and under different conditions of melt cooling, either by rapid quenching in water at 23°C, or after allowing the 4-mm diameter polymer extrudate to cool more slowly in air to room temperature. Some samples were also made with additions of 10% by weight of sized short glass fiber reinforcement, blended with the ε-caprolactam/catalyst/activator feedstock, in order to investigate possible effects from additive nucleation on the crystalline microstructure.

IR Spectroscopy

The chemical structure of the materials produced was examined in absorbance mode by Fourier transform infrared spectroscopy (FTIR), using thin films ($\approx$ 5-μm thick). A comparison was made with PA6 produced by hydrolytic polymerization (available commercially as CAPRON 8202C, Allied Chemicals Inc.), and also with the ε-caprolactam monomer.

WAXD

Analysis of the crystalline order in the PA6 was undertaken by WAXD using a Phillips PW1050 go-

niometer at 23°C, through diffraction angles (2Θ) from 8–30° with nickel filtered copper K_α radiation. Specimens used were in the form of thin strips ($\approx$ 1-mm thick) cut normal to the long axis of the extruded rod.

Before characterization, residual monomer was extracted from materials by immersion in distilled water for 12 h at 100°C followed by drying under vacuum for 24 h at 110°C. In some cases, samples were also annealed at 180°C for 90 min *in vacuo* prior to analysis.

Thermal Analysis

PA6 samples were analyzed on a Perkin–Elmer DSC-2B differential scanning calorimeter, under controlled conditions of heating and cooling, to assess melting and recrystallization behavior. This was carried out in three steps. In stage I, 5–10 mg of material was taken from a section perpendicular to the direction of extrusion and heated from room temperature to 250°C at a rate of 10°C min^{-1}, to investigate sample melting. After maintaining the temperature at 250°C for 15 min, polymer was cooled to 40°C at 5°C min^{-1} (stage II) to determine its recrystallization temperature. In stage III, a second melting endotherm was then obtained using the same conditions as in the initial heating step. As with WAXD analysis, before testing some samples were also annealed at 180°C for 90 min *in vacuo*.

All DSC experiments were conducted in sealed aluminum pans in a nitrogen atmosphere. From the energy changes produced, data were collected for maximum melting and crystallization changes, together with heats of fusion (ΔH_f), from which the degree of crystallinity was calculated.

Dynamic Mechanical Analysis (DMA)

The thermomechanical properties of PA6 were obtained from analysis of rod extrudate, using a Rheometrics RSA II dynamic mechanical analyzer. Samples were tested in a three-point bending mode over a heating range of −100–130°C, using a frequency of 6.28 rad s^{-1} (1 Hz). Elastic storage modulus (E') and damping loss factor ($\tan \delta$) were recorded as a function of temperature.

Testing was undertaken in a three-point flexural mode, with specimens in the form of 4-mm diameter rods produced from the extruder. In most samples, residual monomer was extracted by conditioning the material in boiling water for 12 h before drying at 110°C for 24 h. Specimens were then stored for 72

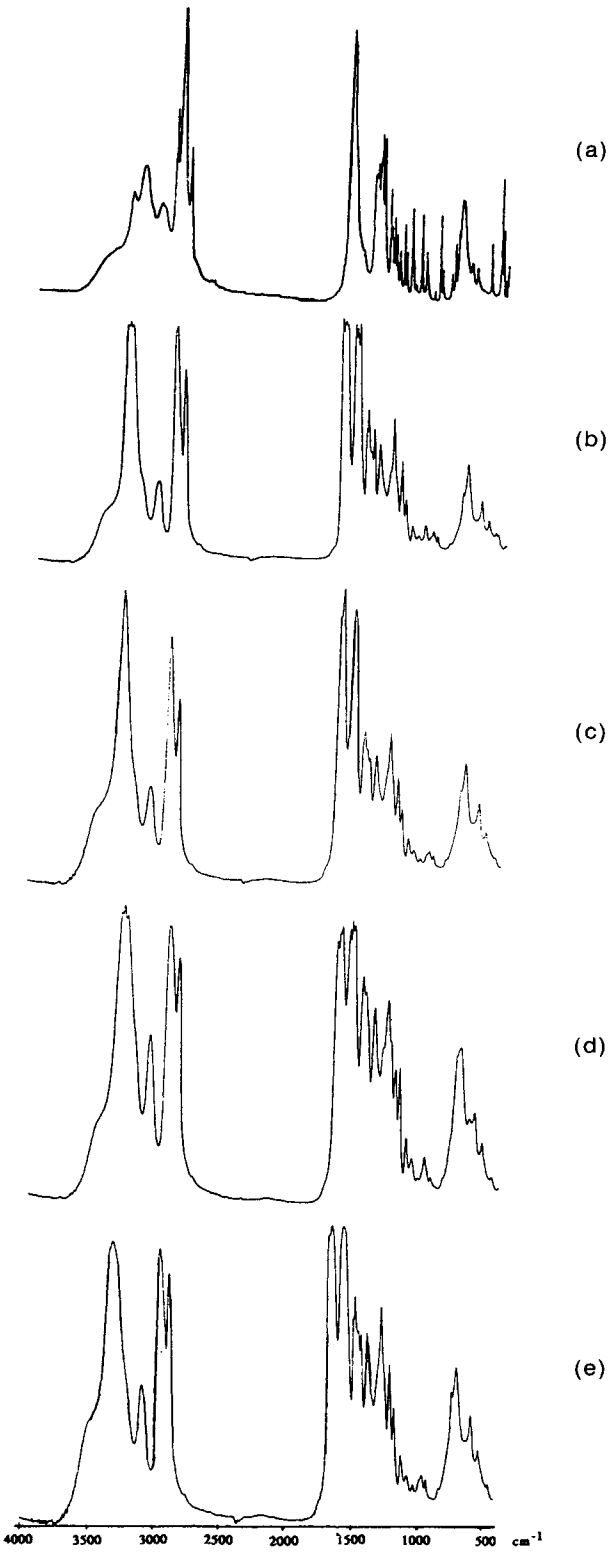

Figure 1 FTIR spectra of PA6 variants and caprolactam monomer: (a) ϵ-caprolactam; (b) commercial PA6 (Capron 8202C); (c) PA6 extruded at 50 rpm; (d) PA6 extruded at 90 rpm; (e) PA6 extruded at 150 rpm.

h at 50% relative humidity (RH) (23°C) before testing. Some PA6 containing residual monomer was also analyzed for comparison.

RESULTS AND DISCUSSION

Figure 1 compares TIR spectra for PA6 made by reactive extrusion at different screw speeds with results obtained from commercial material and ϵ-caprolactam monomer.

Table I lists likely assignments to these absorption bands of PA6 variants. Close agreement is observed although slight differences in the intensity and position of certain absorption bands can be detected, which may be related to the polymer molecular weight. For example, an intense band at around 3302 cm^{-1} is assigned to the hydrogen-bonded NH stretching amide band with two associated satellite absorptions occurring at 3200 and 3062 cm^{-1}. The principal NH band occurs at 3301, 3300, and 3286 cm^{-1} corresponding to PA6 weight-average molecular masses of 53.7, 60.5, and 140 kg mol^{-1}, for polymer prepared at the different screw speeds. Commercial PA6 (M_w = 25.1 kg mol^{-1}) exhibited an intense band at 3308 cm^{-1}. The observed decline in the position of this band to lower wave numbers appears to follow the increase in molecular mass of reaction extruded samples and the resulting increase in interchain hydrogen bonding that ensues. Ismat[4] also reported similar shifts in the position of the amide group absorption in PA6/iodine complexes as compared to unmodified PA6 made by hydrolytic polymerization.

CH_2 stretching bands at 2933, 2936, and 2944 cm^{-1} for PA6 prepared at screw speeds of 50, 150, and 90 rpm, respectively, show an increase in frequency of absorption with increasing sample molecular mass. The corresponding absorption for commercial PA6 was detected at 2932 cm^{-1}. At lower frequencies, additional CH_2 stretching bands at around 1475, 1462, 1439, and 1418 cm^{-1}, were observed for commercial polymer and PA6 prepared at extrusion speeds of 50 and 150 rpm. However, it was noticeable that higher molecular mass material made at 90 rpm yielded only two bands at 1461 and 1441 cm^{-1}.

Positioning CH_2 absorption bands at 1463 and 1440 cm^{-1} have also been observed in PA6/iodine complexes, where in order to accommodate the large I_3^- ion present, the molecules were assumed to take up a zig-zag conformation.[5] Similarly, it is possible that in this study, with very high molecular mass PA6 made by reactive extrusion, chain distortion may occur, resulting in disruption of hydrogen bonding that can produce subsequent changes in the CH_2 stretching absorptions.

The crystalline morphology of PA6 made by reactive extrusion was examined by WAXD and found to be sensitive to preparation conditions, in addition to monomer extraction and annealing procedures adopted.

WAXD profiles of the as-processed water-quenched samples containing residual monomer showed a broad equatorial reflection at around $2\Theta \approx 21.3°$ [Fig. 2(e)]. This suggests the presence of a predominantly γ crystalline morphology with interplanar spacing of $d_{100} \approx 4.2$ Å.[6] However, due to the breadth of this reflection, the presence of α crystallinity cannot be discounted, corresponding to Bragg angles (2Θ) of 19.6 and 23.5° resulting from interplanar spacings of $d_{200} \approx 4.4$ Å and $d_{002} \approx 3.8$

Table I Assignment of FTIR Absorptions for Commercial PA6 and PA6 Made by Reaction Extrusion

	Screw Speed (rpm)			
Band Assignment	50	150	90	Capron
NH Stretching H-bonded/cm^{-1}	3301 (vvs)	3300 (vvs)	3286 (vvs)	3308 (vs)
CH_2 assymm. (aliphatic)/cm^{-1}	2933 (vs)	2936 (s)	2944 (vs)	2932 (vs)
CH_2 symm. (aliphatic)/cm^{-1}	2865 (vs)	2865 (s)	2863 (vs)	2867 (vs)
Amide I, C=O/cm^{-1}	1642 (vs)	1641 (vs)	1630 (vs)	1638 (vs)
Amide II, NH/cm^{-1}	1548 (vvs)	1542 (vs)	1536 (vvs)	1550 (vs)
	1473 (s)	1475 (m)	—	1475 (s)
	1461 (s)	1462 (m)	1461 (vs)	1462 (s)
	1438 (s)	1439 (m)	1441 (vs)	1438 (m)
CH_2 deformation/cm^{-1}	1418 (s)	1418 (m)	—	1418 (s)

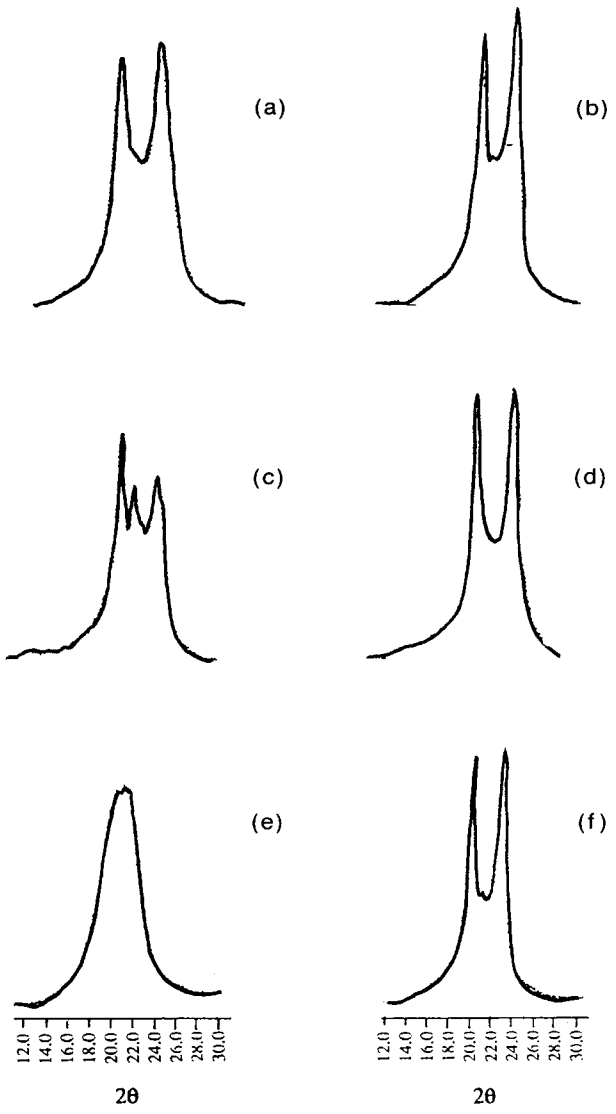

Figure 2 WAXD equitorial profiles of PA6: (a) water quenched, monomer extracted (50 rpm); (b) water quenched/annealed (50 rpm); (c) air cooled with residual monomer (150 rpm); (d) air cooled/annealed (50 rpm); (e) water quenched with residual monomer (50 rpm); (f) commercial PA6; (a)–(e) prepared by reaction extrusion using indicated screw speed; (f) made by hydrolytic polymerization.

Å, respectively.[7] In all water-quenched and most air-cooled samples from which monomer had been extracted after treatment in water, WAXD patterns revealed evidence of only α crystallinity seen, for example, in Figure 2(a), indicating that the γ phase produced originally was unstable to the monomer extraction conditions imposed, subsequently transforming to the more stable α structure.[8] However, because as-processed, air-cooled polymer, containing residual monomer under most preparation conditions, yielded only α-crystalline peaks, it may be inferred that the rate of cooling, and not the presence of monomer, is the dominant factor in determining crystal order and stability, although it was found that air-cooled polymer containing residual monomer made at a screw speed of 150 rpm showed evidence of both α and γ crystalline phases [Fig. 2(c)].

On annealing, the monomer extracted materials at 180°C for 90 min; all water quenched and air-cooled polymer exhibited only α_1 and α_2 crystalline phases on their WAXD profiles with no evidence of γ crystallinity [Fig. 2(b,d)]. Similarly, the WAXD profile of the commercial PA6 used in this work showed characteristic α peaks [Fig. 2(f)], presumably influenced by the nucleating additive believed to be present.[9]

The situation is further complicated by the introduction of short glass fibers during polymerization of the caprolactam. The WAXD profile on reinforced water-quenched material, after monomer extraction, indicates the presence of both α and γ crystalline phases. However, on annealing at 180°C for 90 min, γ crystallinity can still be detected in the structure, in marked contrast to unreinforced PA6 made at 150 rpm using air cooling and tested under identical conditions where, as mentioned previously, the γ crystallinity disappears on annealing.

An explanation of phenomena observed in this study centers around the conditions conducive to the formation of γ rather than α crystallinity and the relative stability of these structures during subsequent treatment or on annealing. It is well established that the α crystalline form of PA6 is in an extended chain conformation whereas in the γ phase, molecules assume a twisted helical arrangement.[10] Furthermore, the α structure is known to be more thermally stable and can be obtained by slow cooling of the melt. It has also been reported that γ crystallinity can exist under stress-induced conditions (as in high speed fiber spinning of PA6), through rapid cooling of the melt as well as by chemical treatment of the α form using iodine.[11] Transformation from γ to α crystallinity can occur either by melting of the polymer followed by slow cooling and recrystallization, or by annealing at temperatures above 160°C.[12]

Complementary structural information can be obtained from examination and analysis of DSC thermograms undertaken on PA6 made by reactive extrusion. Monomer was extracted from all of these materials prior to analysis. Thermal data relating

to melting and crystallization phenomena for selected materials are listed in Table II, with DSC thermograms presented in Figure 3, showing results for the different stages of heating and cooling defined earlier. For the PA6 samples prepared by reactive extrusion, screw speed appeared to have little effect on transition temperatures, hence the results shown are representative values.

Examination of the DSC thermograms reveals that during the first and second heating stages, water quenched material exhibits a relatively broad melting peak, attributed to the gradual fusion of less perfectly formed crystals over an extended temperature range [Fig. 3(a)]. After annealing at 180°C for 90 min followed by slow cooling to room temperature at 23°C, on reheating it was observed that the initial melting peak shows signs of narrowing with only a slight low temperature shoulder, suggesting greater crystal reorganization and perfection has occurred [Fig. 3(b)]. A similar stage I melting transition is evident from analysis of commercial PA6 prepared by hydrolytic polymerization [Fig. 3(d)].

PA6, which was air cooled after extrusion, gave a clear double melting peak during stage I heating, but after annealing at 180°C this reverted to a single melting peak, very similar to the result obtained for water-quenched annealed material shown in Figure 3(b).

When 10% by weight of short glass fibers are present, stage I and stage III melting thermograms show the same trends, as unreinforced PA6. After annealing, however, distinct bimodal melting peaks are seen during stage I heating, which revert to a single peak with a low temperature shoulder during stage II melting [Fig. 3(c)]. It is interesting to speculate that the double melting peaks observed may be due to α and γ forms of crystallinity present.

From the recorded data, all materials prepared by reactive extrusion yielded consistent stage I melting temperatures between 214–216°C, but lower than that obtained for commercial PA6 made by hydrolytic polymerization (Table II). The noticeably higher melting and recrystallization temperature found for the commercial grade of PA6 is attributed to the existence of nucleant believed to be present in this polymer, resulting in the formation of a thermally more stable α crystalline morphology.[9] Heats of fusion and crystallization for PA6, made by reactive extrusion, are broadly similar (particularly for stage III melting), corresponding to about 31–34% crystallinity.

DMA was undertaken on reaction extruded and commercial grades of PA6. Extensive studies on the mechanical relaxation of PAs have been undertaken in recent years, from which it is established that for PA6 there are three relaxation processes in the temperature range −160–200°C, that is α, β, and γ transitions occurring at around 60, −70, and −120°C at a frequency of 1 Hz.[13]

The α relaxation is attributed to the mobility of large chain segments, due to loss of interchain hydrogen bonding as temperature increases, and is considered by many workers to be the glass-transition temperature (T_g) of the polyamide. The β relaxation is associated with crank shaft type motion, involving an unbonded amide group and several methylene carbon groups. The γ transition is a consequence of cooperative motion of methylene groups between amide linkages.

Results for elastic storage modulus (E') and loss factor (tan δ) at 1 Hz, are shown in Figure 4, for PA6 materials obtained commercially and made by reactive extrusion at screw speeds of 70, 90, and 150 rpm, from which residual monomer has been extracted. It is evident that there are two clearly defined mechanical relaxations in the temperature

Table II Thermal Properties of PA6 Variants Made by Reactive Extrusion and Commerical PA6

Sample[a]	T_{m1} (°C)	ΔH_{f1} (Jg^{-1})	T_c (°C)	ΔH_c (Jg^{-1})	T_{m2} (°C)	ΔH_{f2} (Jg^{-1})
Water quenched	214	88	180	58	214	61
Water quenched (annealed)	215	85	180	63	213	64
Air cooled	216	76	181	61	215	62
Air-cooled (annealed)	216	81	181	60	215	66
Capron[b]	221	65	192	65	214	65

T_{m1}, T_{m2} = Peak endothermic melting temperatures, stage I and II heating cycles; T_c = peak exothermic crystallization temperature in cooling cycle; ΔH_{f1}, ΔH_{f2} = heats of fusion, stage I and II heating cycles; ΔH_c = heat of crystallization, cooling cycle.

[a] Reactive polymerized PA6 extruded at 150 rpm.

[b] Commerical PA6 made by hydrolytic polymerization.

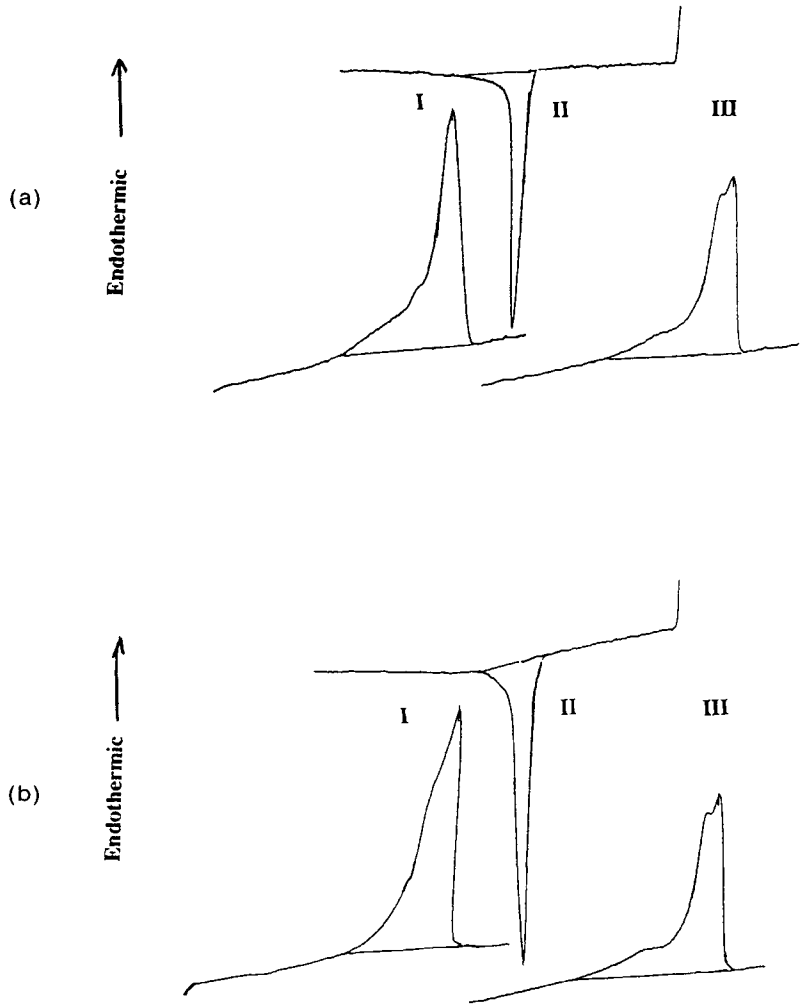

Figure 3 DSC thermograms of PA6 variants: (a) water-quenched PA6; (b) water-quenched/annealed PA6; (c) water-quenched PA6, containing 10% glass fibers/annealed; (d) commercial PA6.

range between −100–130°C corresponding to α and β transitions for PA6. The lower temperature γ transition occurs at a temperature below the range used in this experiment.

The tan δ peak for the glass transition tends to be higher and narrower for PA6 samples prepared at screw speeds of 90 and 70 rpm, compared to material made at 150 rpm, which has substantially lower molecular mass. These observations reflect differences in the extent of interchain hydrogen bonding with variations in chain length.

The commercial PA6 made by hydrolytic polymerization has a T_g at around 60°C, some 10°C higher than that recorded for the PA6 samples made by reactive extrusion. This enhanced T_g value may be attributed to the lower moisture content, as well as slightly higher crystallinity present in the commercial sample tested.

Thermomechanical spectra for reaction extruded PA6, prepared at 150 rpm, then subjected to different preparation conditions are presented in Figure 5. All samples were dried at 110°C for 24 h, then stored in desiccators prior to testing. Water quenched (as processed) extrudate containing 6% of residual monomer gave prominent α and β relaxation transitions at 26 and −73°C, respectively [Fig. 5(a)]. Compared to identical material from which the monomer had been extracted before testing [Fig. 5(b)], the effect of the residual monomer is to reduce the T_g by about 25°C. This observation is in accord with previously reported findings[14] from which it was concluded that residual monomer could function

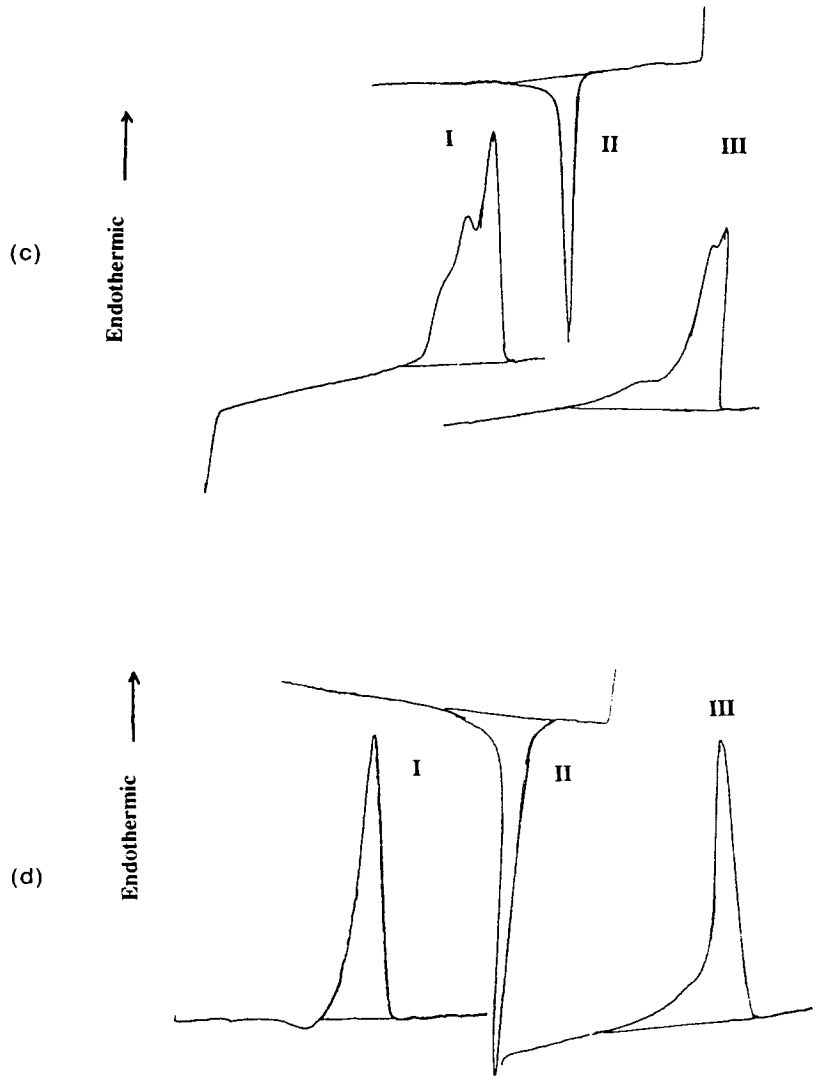

Figure 3 (*Continued from the previous page*)

as a plasticizer in the same manner as combined water. However, both materials yielded approximately the same β transition. This is surprising because water is reported to reduce the temperature of this transition in addition to raising its intensity.

The effect of air cooling PA6 after reactive extrusion is shown in Figure 5(c). It is observed that the air cooled sample has more intense α and β transition peaks than the equivalent water quenched polymer [Fig. 5(b)] and that its T_g is some 10°C higher. No differences were evident in the relative positions of their β transitions, however.

As has been reported in the literature[12] and confirmed earlier in this study, annealing of PA6 at temperatures above 170°C induces a polymorphic transformation from γ to α crystalline morphology. Also, it is known that thermal treatment in this manner can enhance the degree of interchain hydrogen bonding in the structure, producing additional restraints on the molecular mobility of the amorphous region. As mentioned earlier, increased thermal energy will be required to cause dissociation of this hydrogen bonding, which would account for the increased temperature and intensity of the α transition in the annealed PA6 material [Fig. 5(d)].

CONCLUSIONS

It has been demonstrated that PA6 made by anionic polymerization of ϵ-caprolactam in a twin-screw ex-

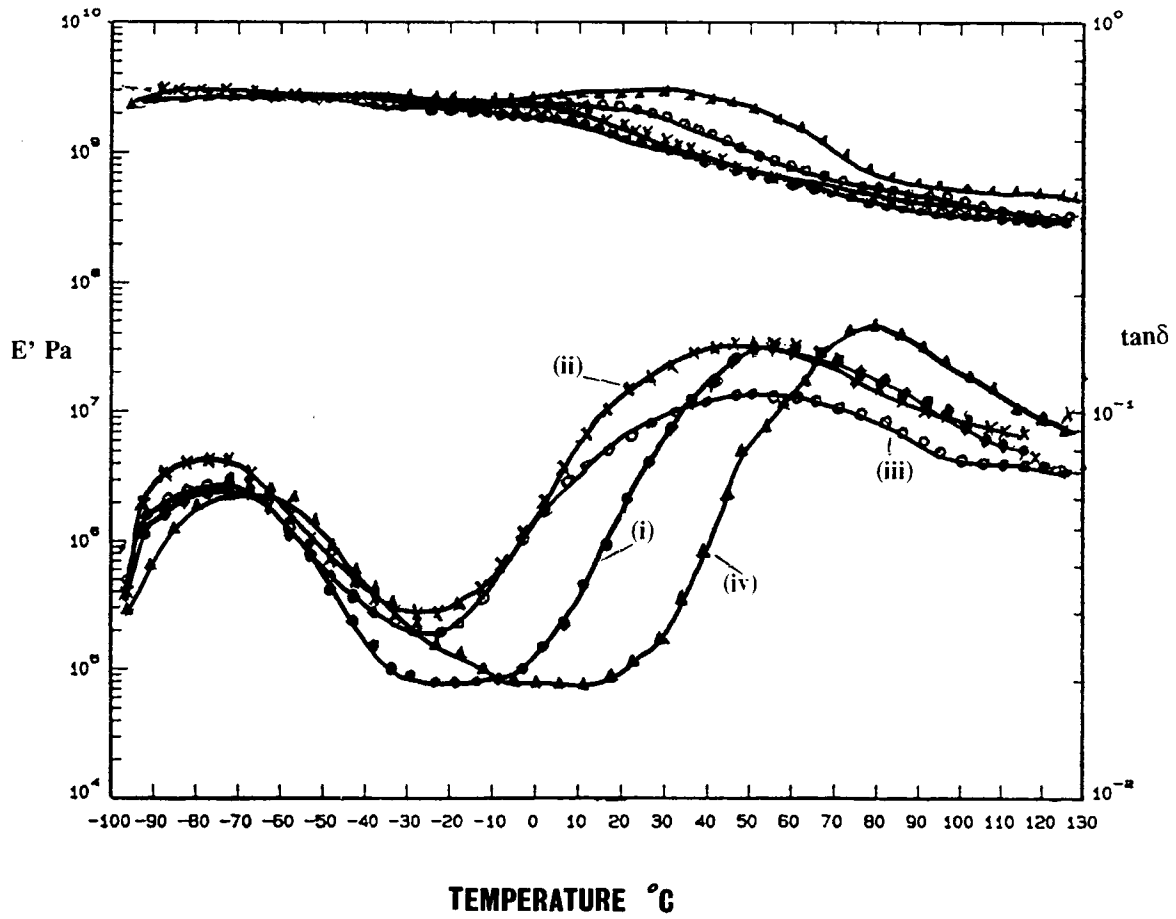

Figure 4 Dynamic mechanical spectra of PA6 variants (a)–(c) made by reactive extrusion at screw speeds of 70, 90, and 150 rpm, respectively (monomer extracted); (d) commercial PA6 made by hydrolytic polymerization.

truder can exhibit microstructural variations according to the conditions of preparation, including polymer molecular mass, thermal history of the material, and the extent of residual monomer present. In general, material produced by this method is quite similar to that polymerized in other reactors.

There was close agreement between IR spectra for PA6 made in the extruder with commercial material produced by hydrolytic polymerization, although with specific absorptions some dependency on molecular mass was seen.

Depending on conditions used to cool the PA6 after preparation, the monomer extraction procedure used and subsequent annealing treatments imposed, different crystalline morphologies were observed. In general, less stable γ crystalline forms were found to transform to more ordered α crystalline morphologies with slow rates of extrudate cooling after monomer extraction in boiling water and following annealing at 180°C in air, although it is significant that PA6 prepared in the presence of reinforcing short glass fibers still retained some γ crystallinity, even after prolonged thermal treatment.

Significantly higher melting and recrystallization temperatures were detected for the commercial polymer compared to PA6 prepared in the extruder, possibly due to the presence of nucleant in the former material.

DMA provided evidence for α and β relaxations in all the PA6 materials studied, although the tan δ peak associated with the glass transition occurred at higher temperatures in polymers of greater molecular mass, reflecting an increase in interchain hydrogen bonding. The presence of residual monomer in the PA6 caused a marked reduction in the temperature of this transition due to polymer plasticization.

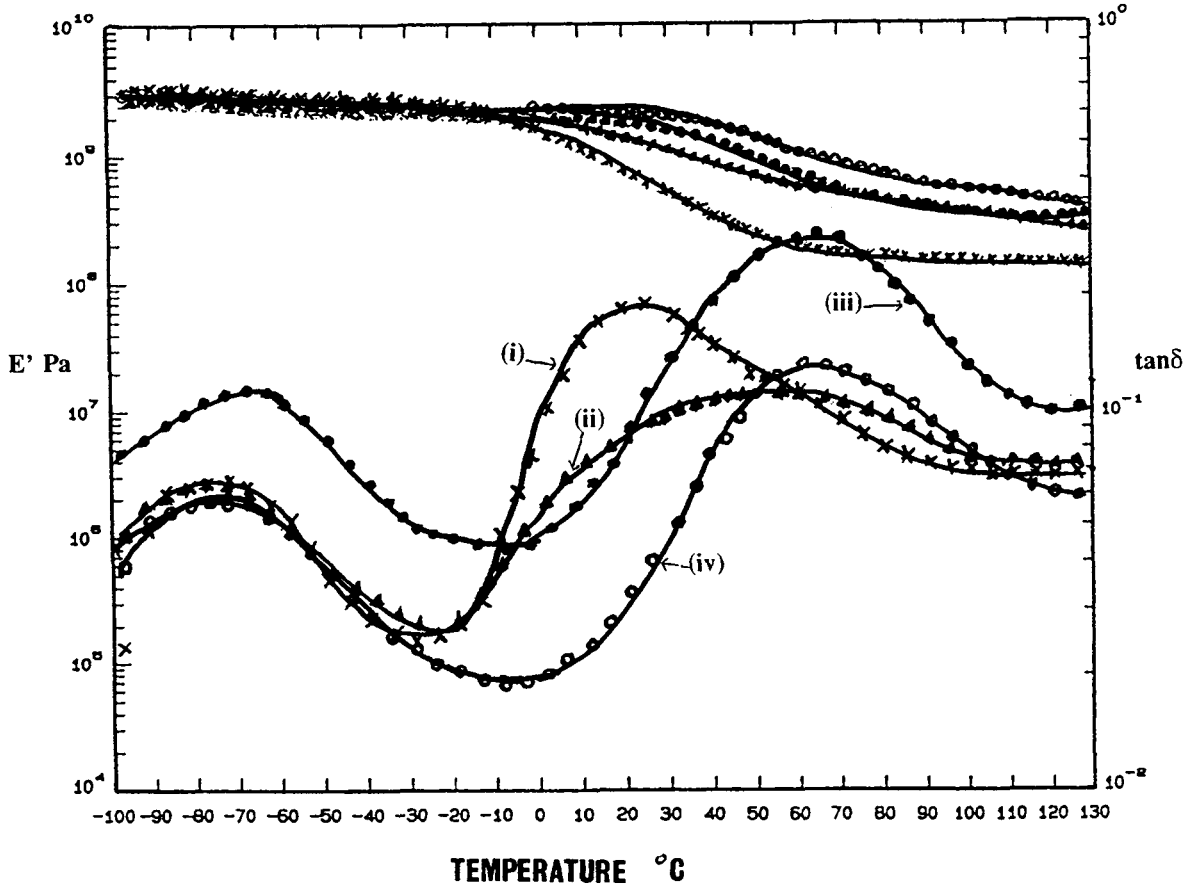

Figure 5 Dynamic mechanical spectra of PA6 subjected to different sample treatments: (i) water-quenched PA6, with residual monomer; (ii) water-quenched PA6, monomer extracted; (iii) air-cooled PA6, monomer extracted; (iv) water-quenched PA6/monomer extracted/annealed.

The authors are grateful to the Standards and Industrial Research Institute of Malaysia for the financial support given to J.F.T.

REFERENCES

1. P. R. Hornsby, J. F. Tung, and K. Tarverdi, *J. Appl. Polym. Sci.*, to appear.
2. J. P. Parker and P. H. Lindenmeyer, *J. Appl. Polym. Sci.*, **21,** 821 (1977).
3. M. Todoki and T. Kawaguchi, *J. Polym. Sci., Polym. Phys. Ed.*, **15,** 1067 (1977).
4. A. Ismat, *J. Polym. Sci. A-1,* **9,** 199 (1971).
5. I. Matsubara and J. H. Magill, *Polymer,* **7,** 199 (1966).
6. M. Kyotani and S. Mitsushashi, *J. Polym. Sci., A-2,* **10,** 1497 (1972).
7. R. Brill, *Phys. Chem.,* **B53,** 61 (1942).
8. D. R. Holmes, C. W. Bunn, and D. J. Smith, *J. Polym. Sci.*, **17,** 159 (1955).
9. Y. Khanna, U.S. Pat. 4,749,736 (1988).
10. H. Arimoto, *J. Polym. Sci., Part A, A-2,* **2,** 2283 (1964).
11. H. K. Illers, H. B. Haberkorn, and P. Sinak, *Makromol. Chem.*, **158,** 285 (1972).
12. N. S. Murthy, S. M. Arohoni, and A. B. Szollosi, *J. Polym. Phys. Ed.*, **23,** 2549 (1985).
13. V. B. Rele and Y. S. Papir, *J. Macromol. Sci.-Phys. B* **13**(3), 405 (1977).
14. C. Garbuglio, G. Ajroldi, T. Casiraghi, and G. Vittadiai, *J. Appl. Polym. Sci.*, **15,** 2487 (1971).
15. T. J. Bessell, D. Hull, and J. B. Shortall, *J. Mater. Sci.*, **10,** 1127 (1975).
16. A. Galeski, A. S. Argon, and R. E. Cohen, *Makromol. Chem.*, **188,** 1195 (1987).
17. A. Galeski, A. S. Argon, and R. E. Cohen, *Macromolecules,* **21,** 2761 (1988).
18. J. Martinez-Salazar and C. G. Cannon, *J. Mater. Sci. Lett.*, **3,** 693 (1984).
19. A. Schaper, R. Hirte, C. Ruscher, R. Hillebrand, and E. Walenta, *Colloid Polym. Sci.*, **264,** 649 (1986).
20. R. J. Matyi and B. Crist, *J. Polym. Sci., Phys. Ed.*, **16,** 1329 (1978).

Received December 7, 1993
Accepted May 7, 1994